

Field-dependent dielectric and magnetic properties in multiferroic CdCr₂S₄

C. P. Sun,¹ C. C. Lin,¹ J. L. Her,¹ C. J. Ho,¹ S. Taran,¹ H. Berger,² B. K. Chaudhuri,^{1,*} and H. D. Yang^{1,†}

¹*Department of Physics, Center for Nanoscience and Nanotechnology, National Sun Yat-Sen University, Kaohsiung, 804 Taiwan, Republic of China*

²*Institutes of Physics of Complex Matter, EPFL 1015, Lausanne, Switzerland*

(Received 30 November 2008; revised manuscript received 21 May 2009; published 25 June 2009)

Based on the results of field-dependent dielectric and magnetic measurements, we observe several interesting behaviors and phase transitions in this geometrically frustrated spinel system CdCr₂S₄. (1) A glassy dipolar state occurs near $T_C \sim 85$ K, which is induced by the onset of ferromagnetic ordering. (2) A ferroelectric ordering occurs near $T_p \sim 56$ K, which is enhanced by externally applying electric field. (3) Both the magnitude and step-up temperature of dielectric constant (ϵ') near T_C are suppressed by an electric field yet are increased by the magnetic field. (4) Both electric and magnetic fields colossally enhance the magnitude of dielectric constant (ϵ') near T_p . (5) A clear dip of magnetization under various electric fields is observed near T_p indicating the different spin-dipole interactions near T_C and T_p . Attempts are made to analyze these field-dependent properties by considering the strong spin-lattice coupling and exchange striction effect in this novel multiferroic material.

DOI: [10.1103/PhysRevB.79.214116](https://doi.org/10.1103/PhysRevB.79.214116)

PACS number(s): 77.84.-s, 75.25.+z, 75.50.Dd, 75.80.+q

I. INTRODUCTION

The coexistence of ferromagnetic and ferroelectric (multiferroic) phases in a material has been one of the most attractive issues in fundamental and applied research interests in recent years.¹ Such materials are potential candidates for applications in electronic devices which are operational both by magnetic and electric fields. In order to understand the interaction mechanisms existing among the magnetic moments, the electric dipole and the lattice responsible for the uncommon behavior in such systems are considered as important issues in this fascinating field.²⁻⁴ CdCr₂S₄ was originally discovered as a magnetic semiconductor more than 40 years ago,⁵ and this system drew significant attention due to its important magnetoelectric behavior such as the shift of the absorption edge,⁶ strong spin-lattice coupling, and unusual phonon shift.⁷⁻⁹ The evidence showed that the magnetic ordering in chromium chalcogenide spinels was strongly coupled with dielectric and optical properties. The strong spin-lattice (phonon) coupling had been considered to be responsible for the change in phonon spectrum by magnetic ordering and had also been reported to lead to a local lattice distortion appearing with the magnetic ordering.^{10,11} Recently it was claimed by Hemberger *et al.*¹² that CdCr₂S₄ exhibits multiferroic behavior with evidence of relaxor ferroelectricity and colossal magnetocapacitance. Catalan and Scott,^{13,14} however, suggested an alternative explanation of the relaxor behavior in CdCr₂S₄ that it might possibly be related to extrinsic properties such as chlorine-based impurities or sulfur deficiency. Because of such concerns,¹²⁻¹⁴ one group recently reproduced the result of magnetocapacitive effect on a new single crystal synthesized using bromine gas, instead of chlorine gas, as a transport agent. Also it was suspected that bromine is hardly to enter the lattice.¹⁵ Therefore, these multifunctional properties encouraged us to study the temperature, electric-field-dependent and magnetic-field-dependent magnetization, and dielectric constant on this novel CdCr₂S₄ system to investigate the conflicting interpre-

tations. In this paper we present several features which support the evidences of multiferroic interaction in CdCr₂S₄ under the application of external electric and magnetic fields.

II. EXPERIMENTAL METHODS

Single crystals of CdCr₂S₄ were grown by chemical vapor transport from the synthesized powder. The primary reaction products were enclosed in evacuated (10^{-6} Torr) and sealed silica ampoules (a length of about 200 mm and an inner diameter of 32 mm) along with electronic grade Cl₂ gas and CrCl₃ as transporting agents. The ampoules were then heated in two-zone gradient furnace. The optimal temperatures at the source and deposition zones were between 900 and 850 °C, respectively. The two single crystals grown from two independent batches were checked by magnetization and specific-heat measurements. The checking results showed the exactly identical behavior for two single crystals. For dielectric measurements, the size of the single crystals used was estimated to be about 2 mm × 2 mm × 0.2 mm and silver paint was used as the electrode. The value of applied electric field was estimated by the ratio of voltage to the distance between electrodes. Electric-field-dependent and magnetic-field-dependent dielectric measurements were made under different levels of ac electric fields by using an LCR meter (Agilent 4980A) integrated to the physical properties measurement system from Quantum Design, Inc. All results of the two single crystals are reproducible for each independent cycle. Electric-field-dependent magnetization was carried out by superconducting quantum interference device (MPMS XL-7) magnetometer and the direction of electric field was applied perpendicular to the magnetic field.

III. RESULTS AND DISCUSSION

The frequency-dependent dielectric constant at fixed electric field 10 V/cm is plotted in Fig. 1. The observed enhancement of dielectric constant just below the ferromagnetic or-

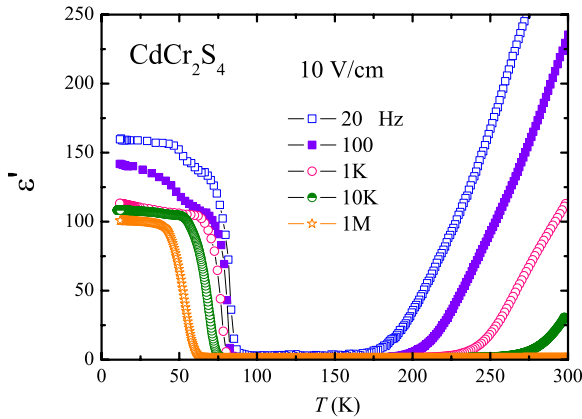


FIG. 1. (Color online) Frequency-dependent dielectric constant is measured at fixed ac electric fields (10 V/cm). No evidence of relaxor behavior is observed between 150 and 250 K. Two single crystals from different batches show an identical behavior.

dering transition temperature $T_C \sim 85$ K is strongly correlated with ferromagnetic ordering and also consistent with the previous report.¹² Exchange striction, which mechanically induces the strain, is associated with the ferromagnetic ordering around T_C and local lattice distortion takes place inducing the enhancement of dielectric constant.¹⁰ The crucial role of the exchange striction in this system has been previously noted.^{10,12} It is somewhat surprising that the relaxor behavior appearing in the high-temperature region (180–250 K) as reported in Ref. 12 is not observed in Fig. 1 of the present dielectric measurement. In the present study, two independently grown single crystals were used and both were found to show identical behavior confirming the reproducible data and the good quality of our samples. Therefore, whether the existence of high-temperature (~ 180 K) relaxor behavior reported¹² recently is an intrinsic or extrinsic feature needs further clarification.^{13,14} Detailed information of crystal growth has been described in the experimental methods.

Dielectric constant measured under different ac electric fields from 10 to 100 V/cm and at a frequency of 20 Hz is shown in Fig. 2(a). With increasing external electric field we clearly observe two interesting phenomena. First, the gradual decrease in the ferromagnetically stimulated step-up dielectric constant around $T_C = 85$ K indicates a highly disordered or glassy-type dipolar state. Martin *et al.*¹¹ proposed that below T_C the system is magnetically inhomogeneous due to the competing phase of superexchange, where the nearest-neighbor (NN) Cr-S-Cr spins contribute to the ferromagnetic coupling, while the next-nearest-neighbor (NNN) Cr-S-Cd-S-Cr spins, more in number and further distant, show anti-ferromagnetic interaction. Since the dipoles at temperature near T_C are induced by spin ordering via exchange striction, this leads to the local disordered dipolar ordering and hence glassy-type behavior might appear. To further elucidate the glassy behavior, the frequency-dependent dielectric constant at different temperatures would provide the fruitful information about it and be discussed in Fig. 3. The second phenomenon and the most striking finding shown in Fig. 2(a) is that the electric field enhances a ferroelectric ordering at a lower

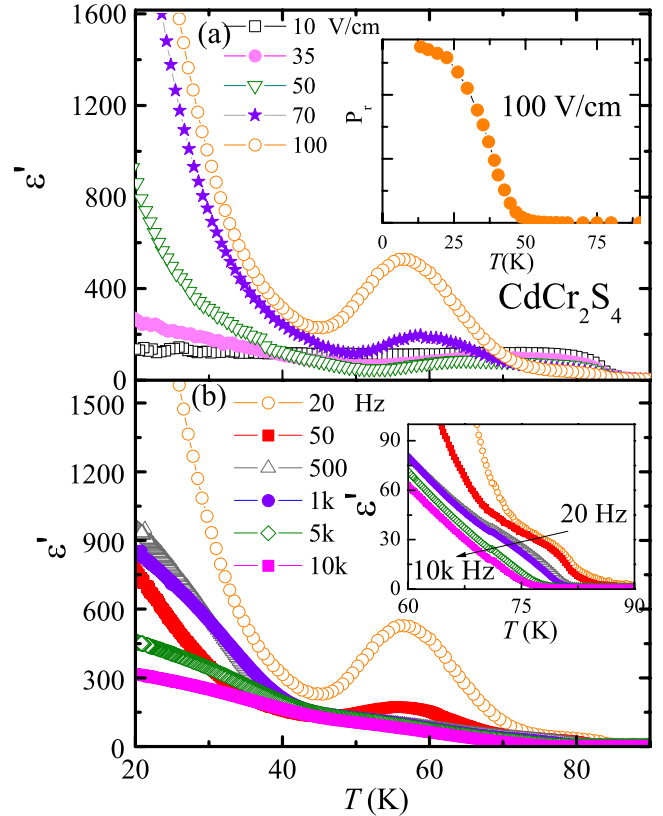


FIG. 2. (Color online) (a) The dielectric constant is measured under different ac electric fields 10 to 100 V/cm at a frequency of 20 Hz and two different transition states are observed: glassy dipolar state near $T_C \sim 85$ K and a ferroelectric ordering state at $T_p \sim 56$ K. The inset shows the temperature-dependent remnant polarization at 100 V/cm supporting the occurrence of a ferroelectric ordering. (b) Frequency-dependent dielectric constants at a field 100 V/cm near T_C and T_p . The enlarged scale near T_C is shown in the inset.

temperature around $T_p \sim 56$ K, which is indicated by the highest peak of dielectric constant observed at a maximum applied field 100 V/cm. This ferroelectric ordering is also supported from the temperature-dependent remnant polarization at the same maximum field, shown in the inset of Fig. 2(a). The electric-field-enhanced ferroelectric ordering suggests that the interaction between spin and dipole around T_p is weaker than that around T_C . When applying the electric field the dipoles align easily along the field leading to a maximum increase in dielectric constant at 56 K. It is noted that dielectric behavior does not depend on applying high dc bias with small ac field or vice versa. We also observe strong frequency dependence of the dielectric constant, as seen from Fig. 2(b) and its inset, where the dielectric constants of both the magnitudes of glassy dipolar state near T_C and ferroelectric ordering near T_p are suppressed with an increase in frequency. These interesting observations under electric field indicate a strong correlation of higher-order lattice vibrations (phonon-phonon interaction) between spins and dipoles in the CdCr_2S_4 system. These observations are also consistent with those reported from the shift in Raman frequency.¹⁶

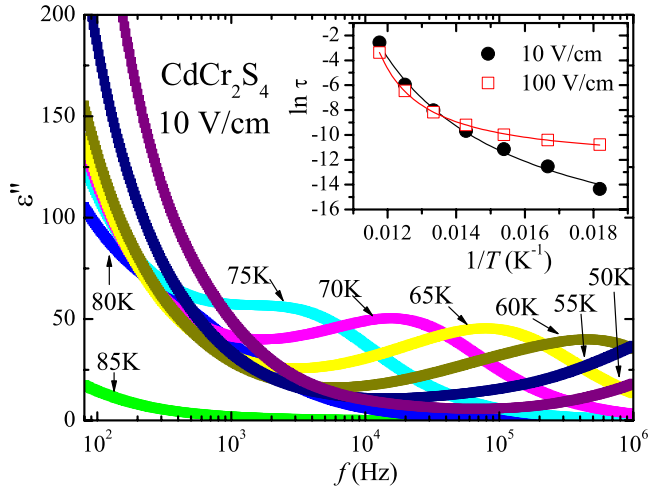


FIG. 3. (Color online) The imaginary part of dielectric constant (ϵ'') vs frequency is plotted from 85 to 50 K showing the accelerating relaxation behavior with lowering the temperature. Inset shows that relaxation time derived from the dielectric peak follows VF law by the solids lines, which are the best fits to the two sets of data 10 and 100 V/cm, respectively.

In general, the contribution of extrinsic effects such as grain boundary and electrode (the so-called Maxwell-Wagner effect, an interfacial relaxation process) in the field of dielectric spectroscopy is always an important issue to distinguish the authenticity of dielectric phenomena. Because of the natural thermal-activated behavior described by Arrhenius law, linear curve in the plot of logarithm (T) vs $1/T$ will be followed.¹⁷ The thermal-activated relaxation time will be extended as temperature decreases. However, in Fig. 3 we observe that the dipole relaxation time is shorter with lowering temperature, clearly shown by the negative slope of curve in the inset of Fig. 3. The unusual relaxation behavior below T_C is an indication that the Maxwell-Wagner effect is not an origin in describing the new observations and the nonlinear curve in the inset of Fig. 3 doesn't need to be described by the thermal-activated behavior. Based on the results of Figs. 2 and 3, glassy behavior near T_C is suggested by an unusual decrease in dielectric constant near T_C when increasing the electric field and nonlinear curve of relaxation time. To further support it, the relaxation time derived from the frequency dependence of dielectric peak at a temperature range from 85 to 55 K is fitted by the Vogel-Fulcher (VF) law written as $\ln(\tau) = C_1/(T - T_g) + C_2$, where T_g is the freezing temperature and C_1 and C_2 are constants. In general, VF law was used to describe the dynamic properties of systems with glassy state which is attributed to broadening spectrum of relaxation time.^{18,19} This law well fits the experimental $\ln(\tau)$ vs T curve as shown by the solid lines in the inset of Fig. 3 for two sets of data. Best fit to both the electric field data (10 and 100 V/cm) could lead to glassy transition temperature $T_g = 129 \pm 13$ and 96 ± 0.4 K, respectively. The fitting parameters (C_1 and C_2) are -118.5 ± 5.1 K and -13.7 ± 0.1 for 10 V/cm; -1240.6 ± 589.6 K and -30.6 ± 5.2 for 100 V/cm. The well-fitting results further support the glassy behavior in CdCr_2S_4 . We also plot the frequency-dependent imaginary part of electric modulus (M'') within the range of

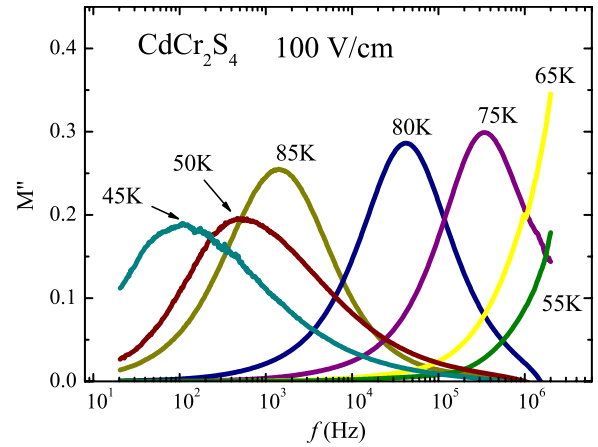


FIG. 4. (Color online) The imaginary part of electric modulus (M'') vs frequency is plotted for the temperature between T_C and T_p . Alternative evidences support the unique and intrinsic properties in CdCr_2S_4 .

phase transition temperatures (T_C and T_p) in Fig. 4. Electric modulus (M') is defined as $M^* = M' + iM'' = i\omega C_0 Z^* = \frac{1}{\epsilon^*} = \frac{1}{\epsilon' - i\epsilon''}$, where ω is the angular frequency and $C_0 = \frac{\epsilon_0 A}{d}$ is the empty cell capacitance (A is the electrode area and d is the separation between electrodes). Electric modulus is usually compared with the impedance (Z) and permittivity (ϵ) to investigate the microscopic relaxation process, which could be also used to analyze the contribution of grain and grain boundary in a dielectric system.²⁰ Therefore, the results of Fig. 4 again support several important issues in these new observations in CdCr_2S_4 . First, the slowing relaxation properties could be also observed in the range between $T_C \sim 85$ K and $T_p \sim 56$ K, where the relaxation time is shorter as the temperature is lowered from 85 to 55 K. Below 55 K, the relaxation behavior returns back to normal case in which relaxation time is longer as temperature decreases. It supports the existence of phase transition below 55 K ($\sim T_p$) that a ferroelectric ordering state is enhanced by electric field. Second, the magnitude of the M'' peaks in the temperature range from 85 to 45 K is following different trends. Above T_p the magnitude is gradually increasing, however, it is lowering below T_p . This result is associated with the occurrence of polarization shown in the inset of Fig. 2 because the magnitude of M peak is relevant to the capacitance of the investigated system. The capacitance value of grain and grain boundary in the system is usually different.²¹ Therefore, the possibility of extrinsic effects such as grain boundary or impurity existing in single crystals studied could be neglected and new observations enhanced by electric field could be related to the intrinsic properties in the present system.

The importance of spin-lattice coupling in the present system is further indicated from the temperature-dependent magnetization measurement under electric field as shown in Fig. 5. A strong reduction in magnetization is observed well below $T_C \sim 85$ K with increasing external dc electric field. A new and remarkable feature is that the external electric field induces a dip in the $M(T)$ curve at 54 K which gradually grows deeper and clearer as the electric field increases. The

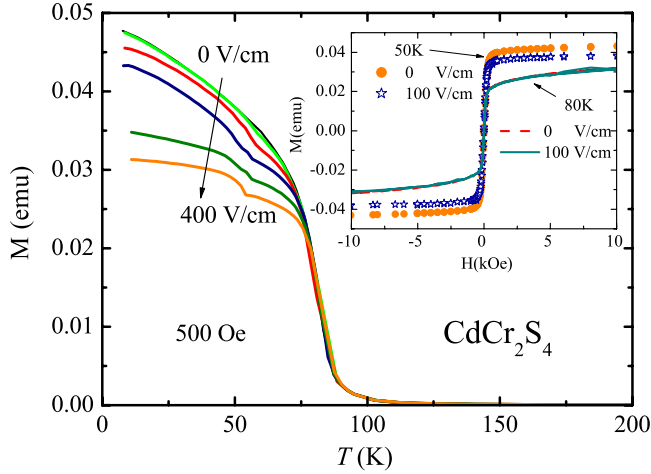


FIG. 5. (Color online) Temperature-dependent magnetization is measured at 500 Oe. A dip near T_p becomes gradually clearer with increasing external dc electric field. The inset shows the isothermal $M(H)$ at 80 and 50 K at electric fields of 0 and 100 V/cm. Suppression of $M(H)$ by electric field is seen at $T=50$ K (below T_p), but not observed at $T=80$ K (below T_C).

temperature of the dip is corresponding to the peak temperature T_p of dielectric constant under various electric fields shown in Fig. 2(b). These newly discovered phenomena shown in Figs. 2 and 5 can be explained to be due to the strong correlation among magnetic spin, electric dipole, and the lattice in CdCr_2S_4 . The inset of Fig. 5 shows the isothermal magnetization measurement taken at 80 and 50 K (below T_C and T_p , respectively) which indicates no detectable suppression of magnetization by an electric field as high as 100 V/cm at 80 K, but a countable suppression occurs at 50 K. These observations also distinguish two types of dipolar ordering behaviors in CdCr_2S_4 : one is the so-called glassy dipolar state near $T_C \sim 85$ K and the other is the ferroelectric ordering around $T_p \sim 56$ K as discussed in Fig. 2. To better understand the relationship between dipoles and spins it is essential to study the magnetic-field-dependent dielectric constant.

Figure 6 shows that the dielectric constant at both glassy dipolar state and ferroelectric ordering phase is enhanced by magnetic field and shows significant colossal behavior. It is important to mention that if we calculate the magnetocapacitive ratio at magnetic field 5 T (the ratio is defined as $\Delta\epsilon'/\epsilon'(0 \text{ T}) = [\epsilon'(5 \text{ T}) - \epsilon'(0 \text{ T})] / \epsilon'(0 \text{ T}) \times 100\%$) for the glassy dipolar state near T_C (shown in the inset of Fig. 6), this ratio comes out to be $\sim 500\%$, which agrees well with that reported in Ref. 12. However, the ferroelectric ordering near T_p under magnetic field shows a much higher ratio than that of the corresponding glassy dipolar state. This colossal magnetocapacitive behavior might be due to the fact that under magnetic field, spins are more ordered and the exchange striction is further enhanced. It is also observed that the dielectric constant step-up temperature (T_C) is increased with magnetic field as shown in the inset and also strongly associated with the ferromagnetic ordering under magnetic field. However, the peak temperature T_p associated with ferroelectric ordering is slightly lowered by magnetic field.

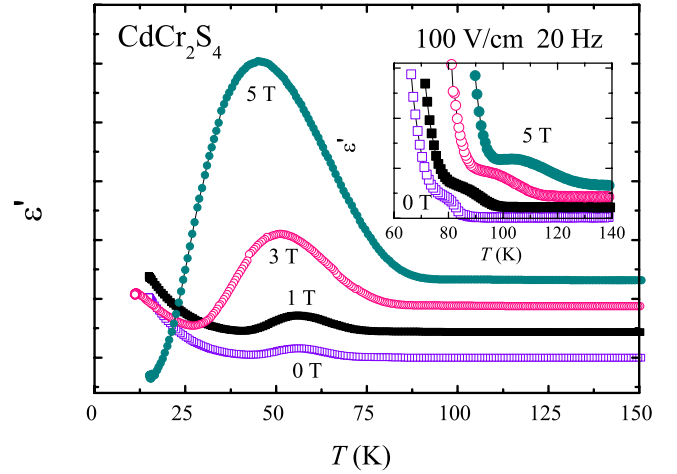


FIG. 6. (Color online) The position of glassy dipolar state ($\sim T_C$) is shifted to high temperature with increasing magnetic field; however, ferroelectric ordering temperature (T_p) is slightly suppressed. Dielectric constant of both states is colossally enhanced by external magnetic field but it is much more heightened near T_p than near T_C . Inset provides a clear indication of dielectric constant near T_C under different magnetic fields. The value of vertical axis for each curve is offset by 20% for clarity.

Therefore, spin-lattice coupling assisted by magnetic field clearly shows the distinct interactions between spin and dipole, which lead to two different behaviors of the dielectric constants near T_C and T_p . Because the crystals used are not of the rectangular shape, the electric field is not exactly parallel or perpendicular to the magnetic field. In fact, different runs of measurements with different samples and electrode connection configurations get a similar behavior. In addition, CdCr_2S_4 has a spinel cubic structure. Thus, the direction of the electric field to the magnetic field would not much affect the dielectric behavior we observed in the present study. The frequency-dependent dielectric constant at constant magnetic field (3 T) is plotted in Fig. 7. The magnitude of ferroelectric peak near T_p is strongly suppressed when frequency increases and the relaxation behavior near T_C is consistent with

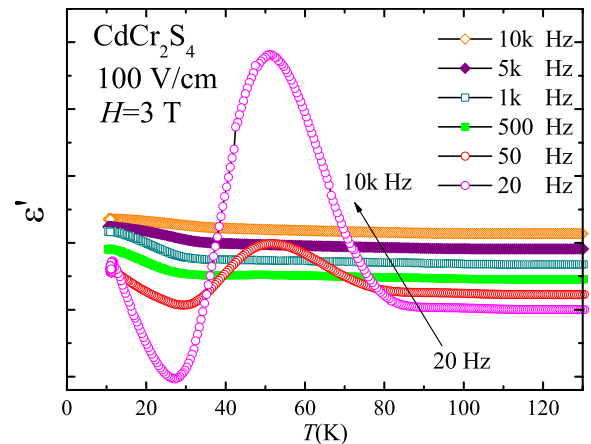


FIG. 7. (Color online) The colossal magnetocapacitance is suppressed by increasing the applied frequency from 20 to 10 kHz. The value of vertical axis for each curve is offset by 40% for clarity.

the case shown in the Fig. 2(b). The observation of magnetocapacitive peak suppressed by increasing frequency could be compared with the published results of other ferroelectric materials.²² From the extrinsic point of view, to investigate the colossal magnetocapacitive effect in the present system, the previous report²³ indicated that the magnetodielectric effect could also have occurred without magnetoelectric coupling. It could have resulted from the combination of magnetoresistance and the Maxwell-Wagner effect. However, this assumption is not enough to describe these new field-dependent observations based on the results of Figs. 3 and 4. Therefore, the colossal electrocapacitive and colossal magnetocapacitive effects in the present system should be paid more attention to investigate its essence.

According to the case of Rochelle salt,²⁴ a strong spin-phonon coupling in a two-sublattice system explained by an asymmetric double-well potential has previously been proposed.^{25,26} Interestingly, such a two-sublattice model with strong spin-phonon coupling indicates the presence of two transitions: one transition [$T_{C1} \approx f(V, J, K)$] is related to the spin-phonon coupling constant (V , containing higher-order phonon-phonon interaction constants) and the spin-spin exchange constants (J and K), and the other [$T_{C2} \approx f(J, K)$] is a function of only pure spin-spin exchange constants.¹⁶ The two-sublattice picture for the CdCr_2S_4 system with spin-spin interaction constants (J and K for different sublattices, respectively) was considered earlier by Wakamura *et al.*,⁷ but the direct spin-phonon interaction has not been proposed before. This two-sublattice picture might also be used to describe the complicated phonon spectrum and phase transitions in the present CdCr_2S_4 system where there is strong coupling of a two subspin systems (NN and NNN) with the lattice. The strength of the spin-lattice coupling in the two subspin systems is not the same, and both are magnetic and electric field dependent due to the exchange striction (a consequence of strong spin-phonon and phonon-phonon interactions). This is associated with spin ordering between the Cr ions in the cubic cell and which might lead to a local anomalous volume increase or decrease.^{27,28}

Moreover, a recent review article²⁹ proposed that the nature of ferroelectricity in the so-called “type II” multiferroic material can be induced by the strong coupling with the magnetic spin through exchange striction. The present results are consistent with the hypothesis. Therefore, the effect of exchange striction is clearly significant both in electric and magnetic fields and is responsible for the different magnetoelectric phenomena exhibited in CdCr_2S_4 .

IV. SUMMARY

In summary, there are several findings presented in this paper. (1) A glassy dipolar state below $T_C \sim 85$ K which is strongly associated with ferromagnetic ordering and an electric-field-enhanced ferroelectric ordering at $T_p \sim 56$ K, are for the first time clearly identified in CdCr_2S_4 . (2) Both the magnitude and step-up temperature of dielectric constant (ϵ') near T_C are suppressed by an electric field yet are increased by a magnetic field. (3) Both electric and magnetic fields colossally enhance the magnitude of dielectric constant (ϵ') near T_p . (4) The magnetodielectric effects near T_C and T_p indicate the different spin-dipole coupling mechanisms responsible for these two transitions. These observations derived from the frequency, electric-field-dependent and magnetic-field-dependent dielectric constant, and magnetization are rather unique among multiferroic materials. A further understanding of the complicated coupling mechanism and its possible application is necessary and deserves continuing investigation in this interesting spinel multiferroic CdCr_2S_4 system.

ACKNOWLEDGMENTS

This work was supported by National Science Council of Taiwan, R.O.C. under Grant No. NSC 97-2112-M110-005-MY3.

*Permanent address: Department of Solid State Physics, Indian Association for the Cultivation of Science, Kolkata, West Bengal 700032, India.

†Corresponding author; yang@mail.phys.nsysu.edu.tw

¹W. Eerenstein, N. D. Mathur, and J. F. Scott, *Nature* (London) **442**, 759 (2006).

²T. Kimura, T. Goto, H. Shintani, K. Ishizaka, T. Arima, and Y. Tokura, *Nature* (London) **426**, 55 (2003).

³D. L. Fox and J. F. Scott, *J. Phys. C* **10**, L329 (1977).

⁴N. A. Hill, *J. Phys. Chem. B* **104**, 6694 (2000).

⁵P. K. Baltzer, H. W. Lehmann, and M. Robbins, *Phys. Rev. Lett.* **15**, 493 (1965).

⁶G. Harbeke and H. Pinch, *Phys. Rev. Lett.* **17**, 1090 (1966).

⁷K. Wakamura and T. Arai, *J. Appl. Phys.* **63**, 5824 (1988).

⁸H. W. Lehmann and M. Robbins, *J. Appl. Phys.* **37**, 1389 (1966).

⁹P. K. Baltzer, P. J. Wojtowicz, M. Robbins, and E. Lopatin, *Phys. Rev.* **151**, 367 (1966).

¹⁰T. Rudolf, Ch. Kant, F. Mayr, J. Hemberger, V. Tsurkan, and A. Loidl, *Phys. Rev. B* **76**, 174307 (2007).

¹¹G. W. Martin, A. T. Kellog, R. L. White, and R. M. White, *J. Appl. Phys.* **40**, 1015 (1969).

¹²J. Hemberger, P. Lunkenheimer, R. Fichtl, H.-A. Krug von Nidda, V. Tsurkan, and A. Loidl, *Nature* (London) **434**, 364 (2005).

¹³G. Catalan and J. F. Scott, *Nature* (London) **448**, E4 (2007).

¹⁴J. Hemberger, P. Lunkenheimer, R. Fichtl, H.-A. Krug von Nidda, V. Tsurkan, and A. Loidl, *Nature* (London) **448**, E5 (2007).

¹⁵S. Krohns, F. Schrettle, P. Lunkenheimer, V. Tsurkan, and A. Loidl, *Physica B* **403**, 4224 (2008).

¹⁶J. Hemberger, T. Rudolf, H.-A. Krug von Nidda, F. Mayr, A. Pimenov, V. Tsurkan, and A. Loidl, *Phys. Rev. Lett.* **97**, 087204 (2006).

¹⁷J. Liu and C.-G. Duan, W. N. Mei, R. W. Smith and J. R. Hardy,

- J. Appl. Phys. **98**, 093703 (2005).
- ¹⁸J. K. Kruger, T. Britz, J. Baller, W. Possart, and H. Neurohr, Phys. Rev. Lett. **89**, 285701 (2002).
- ¹⁹M. Wübbenhorst and J. Jan van Turnhout, J. Non-Cryst. Solids **305**, 40 (2002).
- ²⁰R. Gerhardt, J. Phys. Chem. Solids **55**, 1491 (1994).
- ²¹J. Liu, C.-G. Duan, W.-G. Yin, W. N. Mei, R. W. Smith, and J. R. Hardy Phys. Rev. B **70**, 144106 (2004).
- ²²*Physics of Ferroelectrics*, edited by K. M. Rabe, C. H. Ahn, and J.-M. Triscone (Springer, New York, 2007).
- ²³G. Catalan, Appl. Phys. Lett. **88**, 102902 (2006).
- ²⁴B. K. Chaudhuri, T. Atake, S. Ganguli, and H. Chihara, J. Phys. Soc. Jpn. **49**, 608 (1980).
- ²⁵F. Sandy and R. V. Jones, Phys. Rev. **168**, 481 (1968).
- ²⁶T. Mitsui, Phys. Rev. **111**, 1259 (1958).
- ²⁷M. Shiga and Y. Nakamura, J. Phys. Soc. Jpn. **26**, 24 (1969).
- ²⁸A. Waskowska, L. Gerward, J. Staun Olsen, and E. Malicka, J. Phys.: Condens. Matter **14**, 12423 (2002).
- ²⁹J. van den Brink and D. I. Kohmoskii, J. Phys.: Condens. Matter **20**, 434217 (2008).